IEEE Access
Multidisciplinary Rapid Review Open Access Journal

Received September 3, 2019, accepted September 18, 2019, date of publication September 23, 2019, date of current version October 2, 2019.

Digital Object Identifier 10.1109/ACCESS.2019.2942849

Super-Bandwidth Two-Step Phase-Shifting Off-Axis Digital Holography by Optimizing Two-Dimensional Spatial Frequency Sampling Scheme

BEHNAM TAYEBI[1,2], JEONG HOON PARK[3], AND JAE-HO HAN[1], (Member, IEEE)
[1]Department of Brain and Cognitive Engineering, Korea University, Seoul 02841, South Korea
[2]Department of Biomedical Engineering, Vanderbilt University, Nashville, TN 37235, USA
[3]ITRC Artificial Intelligence Research Center, Korea University, Seoul 02841, South Korea

Corresponding author: Jae-Ho Han (hanjaeho@korea.ac.kr)

This work was supported in part by the Ministry of Science and ICT (MSIT), South Korea, under the Information Technology Research Center (ITRC) support program supervised by the Institute for Information and Communications Technology Planning and Evaluation (IITP) under Grant IITP-2019-2016-0-00464, in part by the National Research Foundation of Korea (NRF) grant funded by the Korean Government under Grant NRF-2017R1A2B2003808, and in part by the LG Yonam Foundation of Korea.

ABSTRACT The presence of the auto correlation and twin cross correlation noises restrict the available spatial bandwidth of the holographic microscopy to much less than the available bandwidth of the digital sensor. Therefore, in order to record the same image area as conventional 2D intensity imaging techniques, several images should be taken. We present two-step phase-shifting off-axis digital holography with maximum space-bandwidth product for three-dimensional (3D) digital holography. Removing the autocorrelation term using a two-step phase-shifting technique significantly increases the available bandwidth for off-axis interferometry. An optimizing super-diagonal two-dimensional (2D) spatial frequency sampling scheme at the sub-Nyquist frequency is employed for performing off-axis interferometry in the absence of the autocorrelation term. The spatial bandwidth of the proposed two-step phase-shifting technique is 400% of that in square scheme off-axis digital holography. Experimental results demonstrate the feasibility of this technique in extracting the 3D morphology of transparent microscopic objects with a larger bandwidth.

INDEX TERMS Holography, interferometry, microscopy, sampling methods.

I. INTRODUCTION

Digital holographic and interferometric microscopy have become promising technologies for generating three-dimensional (3D) topographic information of live cells and nano-scale structures [1], [2]. Both the amplitude and phase of the waves scattered from samples can be obtained by these methods, and the phase information can be used to reconstruct the geometry or compositional structure of transparent objects without requiring an additional labeling process [3]–[5]. Especially, phase-shifting digital holography has played an important role in extracting object phase information from the light intensity measured by a digital camera [6]–[9]. This technique requires four interferograms, which are sequentially or simultaneously recorded. This process dramatically decreases the space-bandwidth product of the digital holography; on the other hand, increasing the sampling rate is an important problem because there are strong physical barriers for the current technologies to increase the pixel number with a constant frame rate. Although two interferograms are considered sufficient for providing the precise phase of the scattered wave [7], this technique requires prior knowledge of the intensity of the reference and object waves. An additional estimation or measurement for the reference field is usually adopted to decrease errors in the retrieved phase of the object [8].

Another technique to extract object phase information is off-axis digital holography that is based on modulation of the scattered signal by a spatial carrier frequency [10]–[12]. Because the phase information in the cross-correlation (CC) term is separated from the intensity information of the auto-correlation (AC) term in the frequency domain, this

The associate editor coordinating the review of this manuscript and approving it for publication was Bora Onat.

technique only requires single-shot recording, enabling high-speed data acquisition compared to phase-shifting digital holography. However, separation of the AC and CC terms significantly restricts the space-bandwidth product. It is demonstrated that the maximum bandwidth for single-shot and single hologram using sub-Nyquist scheme is about 2.44 ($(4/2.56)^2$) times compared to that of conventional off-axis holography using the square sampling scheme [13]. Although several studies claim to have increased the maximum available bandwidth for off-axis holography using multiple sample arms, the maximum bandwidth for single-shot off-axis interferometry with multiple sample arm is experimentally presented in [14]. By using a sub-Nyquist sampling scheme, the available bandwidth area of this technique is more than four times ($2(4/2.71)^2$) that of conventional off-axis holography using the square sampling scheme [14]. However, this technique requires to divide the field of view (FOV) into two FOVs and employ two beams for recording the sample information instead of one sample beam that increases difficulty in alignment. Therefore, despite these recent improvements in the space-bandwidth product of single-shot off-axis holography, the available bandwidth of single-FOV off-axis interferometry is still small compared to the camera bandwidth. Although, Ishizuka [15] demonstrated the optimum sampling schemes for single-FOV off-axis electron holography; however, his schemes for weak scattering objects cannot be applied for optical holographic microscopy with strong scattering objects.

On the other hand, Gross and Atlan [16] suggested a two-step phase-shifting off-axis technique that mapped the frequency domain of strong scattering objects to the frequency domain of the weak scattering objects in the off-axis holography. The technique eliminated the AC term through a two-step phase-shifting method in Mach–Zehnder off-axis interferometry with a low spatial modulation frequency; their technique was employed to increase the spatial sensitivity of off-axis digital holography. Shaked *et al.* [17] employed this two-step phase-shifting technique to increase the bandwidth of the digital holography. Although the available bandwidth of the object phase information is significantly increased and only limited by the twin CC term, the experimental interferogram demonstrated a very low spatial modulation frequency that limited the available to the square sampling scheme bandwidth [17]. Shan *et al.* [18] demonstrated that bandwidth improvement obtained through common-path white-light diffraction-phase interferometry provides better system temporal stability due to the common-path optical configuration. Several other two-step phase-shifting techniques have been presented [19]–[26]; however, these methods have typically focused on system feasibility rather than spatial bandwidth performance.

In this study, we present a super-bandwidth off-axis digital holographic microscopy technique by employing the two-step phase-shifting technique and optimizing the two-dimensional (2D) spatial sampling scheme for recoding the extra information in sub-Nyquist frequencies. First, the two-step phase-shifting off-axis holography of strong scattering objects provides a condition (physically) equal to off-axis holography of weak scattering objects by removing the AC term. Then employing an optimum sampling scheme improves the available bandwidth to half of the available bandwidth of the 2D sensor. The presented technique does not require any prior knowledge of the object intensity. Crosstalk in the frequency domain is avoided because non-occupied frequencies are employed. The experimental results demonstrate at least eight times improvement in the available bandwidth compared to that of previous works with the same number of the images and interferograms [16]–[18].

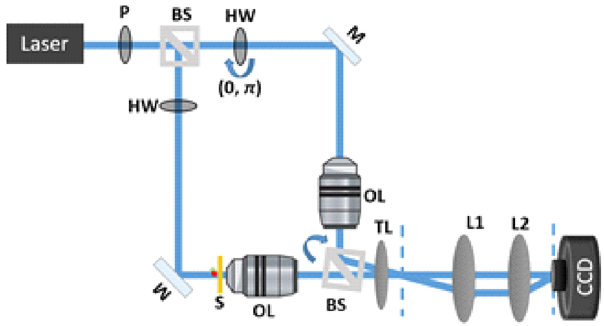

FIGURE 1. Schematic of the two-step phase-shifting off-axis interferometry setup. P: Linear Polarizer, BS: Beam splitter, HW: Half-waveplate, M: Mirror, OL: Objective lens, TL: Tube lens, L1, L2: lens, CCD: charge-coupled device, S: sample.

II. METHODS AND EXPERIMENT

The off-axis phase-shifting digital holography setup is illustrated in Fig. 1. Mach–Zehnder type interferometry, which combines the sample arm and reference arm to form an interferogram at the camera plane, was employed for this experiment. A 405-nm laser beam, which was spatially filtered and linearly polarized, was divided by a beam splitter into two separate optical paths. The sample was illuminated by the laser beam, and a 10× objective lens with 0.3 numerical aperture took a diffraction-limited image at its output port. Two half-waveplates, which were placed before the objective lenses in both the sample and reference arms, created different phase shifts between the two arms. By changing the orientation of the half-waveplate in the reference arm, the phase of the reference field changed, and interferograms with different phases were captured. In order to adjust the diameter of the sidebands in the frequency domain, a 4f optical system was placed before the camera. A charge-coupled device (CCD) camera with 640 × 480 pixels and 4.54 μm pixel pitch captured images with 75 frames-per-second. The recorded intensity can be expressed as:

$$I_\alpha = I_R + I_S + 2\sqrt{I_R I_S}\cos(qx + \beta - \varphi), \qquad (1)$$

where I_R and I_S are the intensities of sample and reference beam, respectively, q denotes the spatial modulation frequency by the angular difference between the sample and reference field, β is the phase shift by the half-waveplate

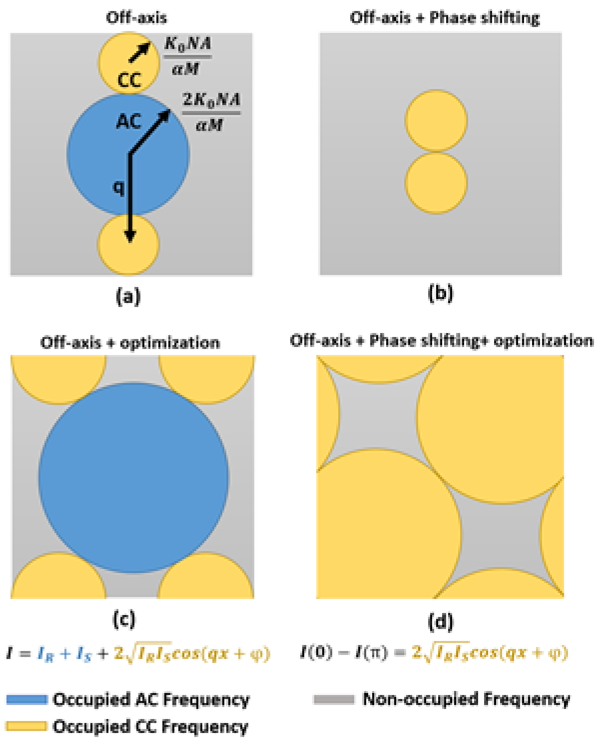

FIGURE 2. Digital frequency domain of: (a) off-axis digital holography with square sampling scheme, (b) previous two-step phase-shifting off-axis interferometric techniques without optimization, (c) off-axis digital holography with optimum sampling scheme, and (d) proposed two-step phase-shifting off-axis digital holography with optimum sampling scheme.

at the reference arm, and φ is the phase of the object. Phase-shifting by half-waveplate rotation at the reference arm induces changes in the intensity. Taking the difference of the interferograms corresponding to the $\beta = 0$ and $\beta = \pi$ phase shifts, we obtain the digitally processed phase image given by

$$I_0 - I_\pi = 4\sqrt{I_R I_S}\cos(qx - \varphi). \quad (2)$$

In (2), the first two terms of (1) or AC terms are removed; therefore, the available frequencies are increased, and a new sampling scheme should be defined to capture the maximum information with this proposed technique.

Fig. 2 compares the different spatial frequency sampling schemes. Off-axis digital holography with square scheme in Fig. 2(a) has the frequency radiuses of $2k_0NA/\alpha M$ for the AC term and $k_0NA/\alpha M$ for the CC term in the spectral domain of the interferogram, where $k_0 = 2\pi/\lambda_0$ is the wavenumber of the illumination source, α is the resolution criterion factor [14], M is the total magnification, and NA is the average numerical aperture of the objective and condenser lenses. To prevent information aliasing between AC and CC, the modulation frequency q must be higher than $3k_0NA/\alpha M$. On the other hand, to digitize each sideband according to the Nyquist frequency, the required digital bandwidth should be twice ($2k$) the maximum bandwidth of that sideband ($k = k_0NA/\alpha M$). Therefore, for Fig. 2(a), the camera bandwidth should be more than $8k_0NA/\alpha M$. Off-axis phase-shifting digital holography in Fig. 2(b) provides the improved bandwidth of the previous two-step phase-shifting off-axis interferometric techniques [16]–[18] compared to conventional off-axis digital holography with square sampling scheme [3]. Since the AC term is removed through subtraction between I_0 and I_π, the only restriction on the modulation frequency is the signal aliasing between CC and the twin CC terms. Thus, the modulation frequency can be decreased from $3k_0NA/\alpha M$ to $k_0NA/\alpha M$. However, the available bandwidth in this scheme is smaller than the maximum available spatial bandwidth for off-axis holography (Fig. 2(c)) [13]–[15], [27]. Fig. 2(d) shows an optimum diagonal sampling scheme for two-step phase-shifting off-axis interferometry. The AC term is removed by the two-step phase-shifting technique, and some parts of the sidebands are recorded in sub-Nyquist spatial frequencies. However, no aliasing occurs because those frequencies were not previously occupied.

The modulation frequency can be controlled by the angle between the reference and sample beams, and the available bandwidth depends on the sensor pixel size. Furthermore, the radius of the sidebands is related to the NA, wavelength, and system magnification. Therefore, a simple way to control the sideband radius is by changing the total magnification of the system. It is demonstrated employing off-axis interferometry, phase-shifting interferometry, or both will not degrade the resolution [12], [16], [18]. Therefore, by applying appropriate magnification, the resolution can be preserved. The magnification of commercial objective lenses is limited; therefore, an additional 4f system is needed to adjust the magnification [14], [27]:

$$M = M_{Obj}M_{4f} = \gamma k_0(NA_{Obj} + NA_{Con})/\alpha K_{cam}. \quad (3)$$

Here, γ is the ratio of the sensor bandwidth to diameter of sideband bandwidth given by where $\gamma = K_{cam}/2k$ where $K_{cam} = 2\pi/P$ is the available bandwidth of the camera in one dimension, P is the pixel size, and $2k$ is the diameter of CC terms in Fig. 2. Further, M_{obj} is the magnification of the objective lens, and M_{4f} is the magnification of 4f optical lens system. Note that γ of the maximum space-bandwidth product in Fig. 2(d) is equal to $\sqrt{2}$. In the proposed technique the modulation frequency, q, is proportional to the inverse of γ. Therefore, for the optical system with circular apertures, the total available frequency area, $\pi(k)^2$, in Fig. 2(d) is half of the total available frequency of the camera with circular aperture (circular area), $\pi K_{cam}^2/4$; we should consider that for comparing the bandwidth area of this technique to single-shot techniques, these values must be divided by a factor of two; because two frames are taken. Therefore, the effective bandwidth area is 0.25 of the total camera bandwidth area with circular aperture. This value for Fig. 2(c) is just $(1/2.56)^2 = 0.15$ for a single frame. These two values compared to total available bandwidth of the camera (square area), K_{cam}^2, are almost 0.196 and 0.12. Therefore, the proposed technique improves the available bandwidth, more than 63% of the sub-Nyquist scheme using a single hologram off-axis interferometric technique [13].

According to our knowledge, the only way to optimizing the spatial frequency sampling scheme in off-axis digital holography is based on geometrical methods that depends on the shape of the sensor pixels and optical apertures. In [14] a figure of merit is defined for comparing the maximum available frequency bandwidth in single-shot off-axis technique. However, the quantity cannot be used for multiple shot technique such as phase-shifting or combination of two techniques such as the proposed technique. Here, we modified this quantity (τ value) for multiple frame techniques that temporally employ more bandwidth and multiple color techniques that have different sideband diameters, because of different resolutions for different colors. The new quantity is called T value and can be expressed as:

$$T = \frac{\pi \sum_{i=1}^{n} w_i k_i^2}{N_{frame} K_{cam}^2} \times 100\% \tag{4}$$

where, ω_i represents the ratio of the non-overlapping area to the total area for the i^{th} hologram, with ω_1 equal to one. k_i indicates the radius of the sideband for i^{th} hologram that is important in color holography with different spatial resolution. Finally, N_{frame} is number of the frame that is required for imaging. Unlike the τ value in [14] that shows the ratio of the available bandwidth of the multiple field of view off-axis holography to maximum bandwidth area of single off-axis holography; the proposed T value shows the ratio of available bandwidth for either inline or off-axis techniques to the maximum bandwidth of the camera (square area). We assumed that the optical apertures are circular and the pixel shape is square; however, this equation can be modified for different aperture and pixel shapes. Therefore, T value for the proposed technique is 19.6%, single hologram off-axis interferometry with sub-Nyquist scheme is 12%, and square sampling scheme is 4.9%.

For a laser source with $NA_{con} = 0$, the magnification of the system can be expressed as

$$M = \sqrt{2} k_0 NA_{Obj} / \alpha K_{cam} = \sqrt{2} P NA_{Obj} / \alpha \lambda. \tag{5}$$

According to (4), for the employed objective lens, the magnification of the 4f system should be 5.75. Therefore, we have selected the magnification of 6, which is closest magnification to 5.75 possible by using combinations of commercial lenses. The modulation frequency equals the sideband's radius (if the sensor's pixels are square) and can be simply adjusted in the Mach–Zander interferometer by tilting the reference beam.

III. RESULTS AND DISCUSSIONS

The feasibility of the proposed technique in removing the aliasing noise for two different cutoff frequencies (windows) was experimentally demonstrated by 3D imaging of polystyrene microspheres with 15, 20, and 30 μm diameters. The refractive index (RI) of the microspheres was 1.627 when immersed in a liquid with RI ~1.604. Fig. 3(a) and (b) show the interferograms of the system background with 0 and π phase shift, respectively. These images were obtained only

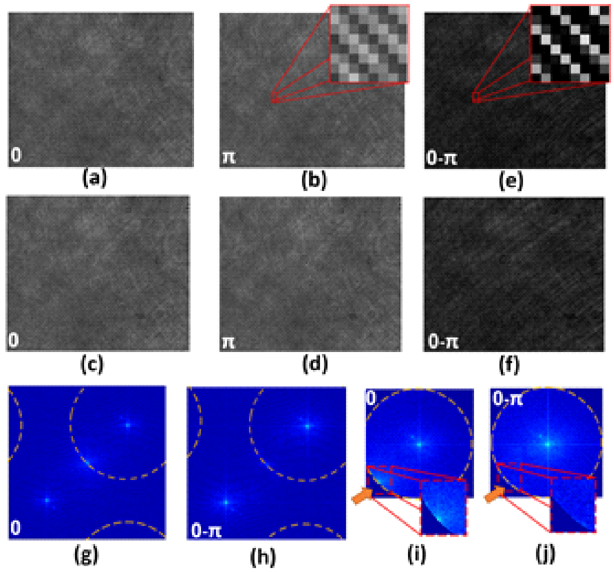

FIGURE 3. **Results of interferograms and Fourier transforms: (a) and (b) are the interferograms of the background of the system with *0* and π phase shift, respectively. (c) and (d) are the interferograms of the sample with *0* and π phase shifts, respectively. (e) and (f) are the interferograms obtained by subtracting the π from *0* phase shift images of the background and sample, respectively. (g) and (h) are the Fourier transform of (c) and (f), respectively. (i) and (j) show the frequency domain of the cropped CC term in (g) and (h), respectively.**

once before starting the experiment to remove the optical path length difference caused by the optical components and background noise. The sample image with *0* and π phase shifts are shown in Fig. 3(c) and (d), respectively. Fig. 3(e) and (f) show the interferograms obtained by subtracting the π phase shift image from the *0* phase shift image for the background and sample images, respectively. The zoomed portions in Fig. 3(b) and (e) show that AC term is properly removed. The Fourier transform of Fig. 3(c) shows a strong AC term that is mixed with CC terms (Fig. 3 (g)). Fig. 3(h) shows the Fourier transform of Fig. 3(f) that indicates an acceptable reduction of the AC frequency. Fig. 3(i) and (j) show the frequency domains of Fig. 3(c) and (f), respectively, after cropping the information with a cut-off circular filter. Although the frequencies are mixed with the AC term in Fig. 3(i), the AC term is appropriately removed in Fig. 3(j) by the two-step phase-shifting technique. Note that the system is very sensitive to the dust and requires an accurate alignment to appropriately remove the effect of the DC [17], [18]. To perform phase retrieval, we employed the Fourier method described in [27] and [28] to obtain the phase, and we used an unwrapping algorithm to resolve any phase ambiguity.

The reconstructed phase of the sample obtained by off-axis interferometry (OI) and by the proposed super-bandwidth two-step phase-shifting off-axis interferometry (SBOI) is shown in Fig. 4. Fig. 4(a) shows the phase of the sample obtained by cropping the spatial frequencies by a window that covers only 60% of the OI object frequencies. This small window reduces the effect of aliasing in OI at the cost of losing 40% of higher frequencies of the sample.

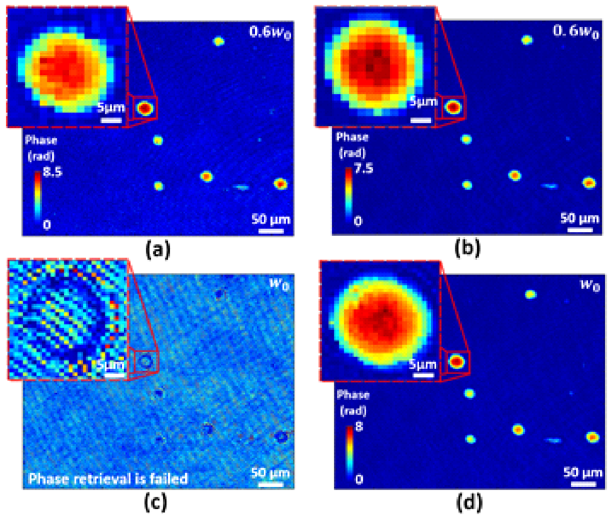

FIGURE 4. Sample results: (a) and (b) are the phases of the sample obtained by cropping the spatial frequencies using a window that covers 60% of the low frequencies for OI and SBOI, respectively. This small window reduces the aliasing effect in OI at the cost of losing 40% of highest frequencies of the sample. (c) and (d) are the phases extracted by employing a full window size to preserve all object frequencies using OI and SBOI, respectively. The OI failed in reconstructing the phase with a super-bandwidth scheme; however, SBOI successfully extracts the object phase.

To compare the effect of this low-pass filtering, we also employed it on the phase obtained by SBOI in Fig. 4(b). In Fig. 4(a), the resolution was degraded compared to Fig. 4(b), and the background noise level was increased. This result occurred because the AC frequencies, found throughout the image, mixed with the CC frequencies in almost all of the available camera bandwidth. Fig. 4(c) and (d) show the extracted phase by employing a full window size to preserve all object frequencies using OI and SBOI, respectively. As shown in Fig. 4(c), OI failed in reconstructing the phase with a super bandwidth scheme because of mixing with the strong frequencies of the AC term. On the other hand, Fig. 4(d) shows that the proposed super-bandwidth technique successfully extracts the object phase. As can be observed in Fig. 4(d), the system preserved higher spatial frequencies that are caused by the defects in the sample. Furthermore, the resolution in Fig. 4(d) is significantly higher than that in Fig. 4(b); although the window size of the filter is larger than the Fig 4(a), the noise level of the system remained low. This result is in a good agreement with the previously reported techniques [17], [18] that mentioned the resolution and sensitivity are preserved in the two-step phase-shifting off-axis holography. The available bandwidth in the proposed technique is improved eight times ($(4/\sqrt{2})^2$) compared to [16]. According to the carrier frequency that is shown in Fig. 3 (b) of [17], it is even more than eight times of the available bandwidth area in [17]. This bandwidth area is also more than eight times than the experimental bandwidth area in [18], it might be because they employed a small carrier frequency for their white light technique to preserve the coherency on the entire field.

IV. CONCLUSION

In summary, we have developed super-bandwidth off-axis interferometry by employing a two-step phase-shifting technique and sampling scheme optimization. The two-step phase-shifting technique removes the AC frequencies that are the main source of restricted bandwidth in off-axis holography. In the absence of the AC term, the optimized diagonal scheme has a bandwidth that is eight times that of previously reported techniques and four times that of single-shot off-axis interferometry with a square scheme. The experimental results of the microscopic transparent samples demonstrate the capability of scan-free imaging, even for critical sampling. The ability to increase the space-bandwidth products without employing more optical components in the setup can significantly improve our vision of microscopic objects. We expect that the proposed technique will open new avenues in high-resolution, large FOV 3D imaging techniques that lack spatial bandwidth.

REFERENCES

[1] V. Bianco, P. Memmolo, M. Paturzo, A. Finizio, B. Javidi, and P. Ferraro, "Quasi noise-free digital holography," *Light, Sci. Appl.*, vol. 5, Mar. 2016, Art. no. e16142.

[2] B. Tayebi, W. Kim, F. Sharif, B.-J. Yoon, and J.-H. Han, "Single-shot and label-free refractive index dispersion of single nerve fiber by triple-wavelength diffraction phase microscopy," *IEEE J. Sel. Topics Quantum Electron.*, vol. 25, no. 1, Jan./Feb. 2019, Art. no. 7200708.

[3] B. Bhaduri, C. Edwards, H. Pham, R. Zhou, T. H. Nguyen, L. L. Goddard, and G. Popescu, "Diffraction phase microscopy: Principles and applications in materials and life sciences," *Adv. Opt. Photon.*, vol. 6, no. 1, pp. 57–119, 2014.

[4] B. Tayebi, J.-H. Han, F. Sharif, M. R. Jafarfard, and D. Y. Kim, "Compact single-shot four-wavelength quantitative phase microscopy with polarization- and frequency-division demultiplexing," *Opt. Express*, vol. 25, no. 17, pp. 20172–20182, 2017.

[5] B. Javidi and E. Tajahuerce, "Three-dimensional object recognition by use of digital holography," *Opt. Lett.*, vol. 25, no. 9, pp. 610–612, 2000.

[6] X. F. Meng, L. Z. Cai, X. F. Xu, X. L. Yang, X. X. Shen, G. Y. Dong, and Y. R. Wang, "Two-step phase-shifting interferometry and its application in image encryption," *Opt. Lett.*, vol. 31, no. 10, pp. 1414–1416, 2006.

[7] J.-P. Liu and T.-C. Poon, "Two-step-only quadrature phase-shifting digital holography," *Opt. Lett.*, vol. 34, no. 3, pp. 250–252, 2009.

[8] E. Cuche, P. Marquet, and C. Depeursinge, "Spatial filtering for zero-order and twin-image elimination in digital off-axis holography," *Appl. Opt.*, vol. 39, no. 23, pp. 4070–4075, 2000.

[9] B. Tayebi, M. R. Jafarfard, F. Sharif, Y. S. Bae, S. H. H. Shokuh, and D. Y. Kim, "Reduced-phase dual-illumination interferometer for measuring large stepped objects," *Opt. Lett.*, vol. 39, no. 19, pp. 5740–5743, 2014.

[10] B. Tayebi, M. R. Jafarfard, F. Sharif, Y. S. Song, D. Har, and D. Y. Kim, "Large step-phase measurement by a reduced-phase triple-illumination interferometer," *Opt. Express*, vol. 23, no. 9, pp. 11264–11271, 2015.

[11] T. Balciunas, A. Melninkaitis, G. Tamosauskas, and V. Sirutkaitis, "Time-resolved off-axis digital holography for characterization of ultrafast phenomena in water," *Opt. Lett.*, vol. 33, no. 1, pp. 58–60, 2008.

[12] B. Tayebi, W. Kim, B.-J. Yoon, and J.-H. Han, "Real-time triple field of view interferometry for scan-free monitoring of multiple objects," *IEEE/ASME Trans. Mechatronics*, vol. 23, no. 1, pp. 160–166, Feb. 2018.

[13] T. Tahara, Y. Awatsuji, K. Nishio, S. Ura, O. Matoba, and T. Kubota, "Space-bandwidth capacity-enhanced digital holography," *Appl. Phys. Express*, vol. 6, no. 2, 2013, Art. no. 022502.

[14] B. Tayebi, F. Sharif, A. Karimi, and J.-H. Han, "Stable extended imaging area sensing without mechanical movement based on spatial frequency multiplexing," *IEEE Trans. Ind. Electron.*, vol. 65, no. 10, pp. 8195–8203, Oct. 2018.

[15] K. Ishizuka, "Optimized sampling schemes for off-axis holography," *Ultramicroscopy*, vol. 52, no. 1, pp. 1–5, 1993.

[16] M. Gross and M. Atlan, "Digital holography with ultimate sensitivity," *Opt. Lett.*, vol. 32, no. 8, pp. 909–911, 2007.
[17] N. T. Shaked, Y. Zhu, M. T. Rinehart, and A. Wax, "Two-step-only phase-shifting interferometry with optimized detector bandwidth for microscopy of live cells," *Opt. Express*, vol. 17, no. 18, pp. 15585–15591, 2009.
[18] M. Shan, M. E. Kandel, H. Majeed, V. Nastasa, and G. Popescu, "White-light diffraction phase microscopy at doubled space-bandwidth product," *Opt. Express*, vol. 24, no. 25, pp. 29033–29039, 2016.
[19] M. Shan, B. Hao, Z. Zhong, M. Diao, and Y. Zhang, "Parallel two-step spatial carrier phase-shifting common-path interferometer with a Ronchi grating outside the Fourier plane," *Opt. Express*, vol. 21, no. 2, pp. 2126–2132, 2013.
[20] N. Sabitov, T. Meinecke, D. P. Kelly, and S. Sinzinger, "Two-step phase-shift interferometry with known but arbitrary reference waves: A graphical interpretation," *Appl. Opt.*, vol. 51, no. 28, pp. 6831–6838, 2012.
[21] J.-P. Liu, T.-C. Poon, G.-S. Jhou, and P.-J. Chen, "Comparison of two-, three-, and four-exposure quadrature phase-shifting holography," *Appl. Opt.*, vol. 50, no. 16, pp. 2443–2450, 2011.
[22] S. Zheng, Y. Cai, X. Pan, X. Zeng, J. Li, Y. Li, T. Zhu, Q. Lin, and S. Xu, "Two-step phase-shifting SPIDER," *Sci. Rep.*, vol. 6, Sep. 2016, Art. no. 33837.
[23] Y. Zhang, X. Tian, and R. Liang, "Random two-step phase shifting interferometry based on Lissajous ellipse fitting and least squares technologies," *Opt. Express*, vol. 26, no. 12, pp. 15059–15071, 2018.
[24] C. Tian and S. Liu, "Phase retrieval in two-shot phase-shifting interferometry based on phase shift estimation in a local mask," *Opt. Express*, vol. 25, no. 18, pp. 21673–21683, 2017.
[25] N.-I. Toto-Arellano, D.-I. Serrano-García, and A. Martínez-García, "Parallel two-step phase shifting interferometry using a double cyclic shear interferometer," *Opt. Express*, vol. 21, no. 26, pp. 31983–31989, 2013.
[26] J.-H. Han, R.-P. Li, J.-H. Liu, F.-S. Hai, and M.-J. Huang, "Two-step phase shifting differential-recording digital holographic microscopy," *Sci. Rep.*, vol. 7, May 2017, Art. no. 1992.
[27] B. Tayebi, Y. Jeong, and J.-H. Han, "Dual-wavelength diffraction phase microscopy with 170 times larger image area," *IEEE J. Sel. Topics Quantum Electron.*, vol. 25, no. 2, Mar./Apr. 2019, Art. no. 7101206.
[28] B. Tayebi, F. Sharif, M. R. Jafarfard, and D. Y. Kim, "Double-field-of-view, quasi-common-path interferometer using Fourier domain multiplexing," *Opt. Express*, vol. 23, no. 20, pp. 26825–26833, 2015.

BEHNAM TAYEBI received the B.Sc. degree in solid state physics from the K. N. Toosi University of Technology, Tehran, Iran, in 2008, the M.Sc. degree in solid state physics from the Iran University of Science and Technology, Tehran, Iran, in 2011, and the Ph.D. degree in applied physics and optics from Yonsei University, Seoul, South Korea, in 2015. From 2015 to 2018, he was a Research Professor with the Department of Brain and Cognitive Engineering, Korea University, Seoul. He is currently a Postdoctoral Scholar with the Department of Biomedical Engineering, Vanderbilt University. His current research interests include optical frequency domain imaging, nanoimaging, holography, interferometry, spectroscopy, signal processing, neuroscience, quantum physics, and solid-state physics.

JEONG HOON PARK received the B.S. and M.S. degrees in ceramics engineering and the Ph.D. degree in materials science and engineering from Seoul National University, Seoul, South Korea, in 1995, 1997, and 2001, respectively. From 2001 to 2017, he was with the SK Hynix R&D Center, Icheon, South Korea, as a Principle Researcher working on thin film technologies for DRAM devices. Since 2017, he has been with the ITRC Artificial Intelligence Research Center, Korea University, where he is currently a Research Corporate Professor. His current research interests include artificial intelligence for advanced device technology and novel optical imaging systems for neuroscience research.

JAE-HO HAN received the B.E. and M.E. degrees in electronics engineering and radio engineering from Korea University, Seoul, South Korea, in 1998 and 2000, respectively, and the Ph.D. degree in electrical and computer engineering from Johns Hopkins University, Baltimore, MD, USA, in 2010. From 2000 to 2005, he was an Associate Researcher with the Fiber Optics and Telecommunications Laboratory, LG R&D Center, Anyang, South Korea. During his Ph.D. studies, he was with the Center of Devices and Radiological Health, U.S. Food and Drug Administration, Silver Spring, MD, USA, in 2008, and also with the IBM Thomas J. Watson Research Center, Yorktown Heights, NY, USA, in 2009, respectively, as a Research Intern. After receiving the Ph.D. degree, he joined the Physical Measurement Laboratory, National Institute of Standards and Technology, Gaithersburg, MD, USA, as a Postdoctoral Associate. Since 2011, he has been with the Department of Brain and Cognitive Engineering, Korea University, where he is currently a Full Professor. His current research interests include artificial intelligence with deep learning methods, intelligent optical sensors for robot-assisted microsurgeries, and novel optical imaging technologies including optical coherence tomography, and microscopy for various fields in nano-biomedicine and neuroscience research.